DOI: 10.2507/34th.daaam.proceedings.xxx

ERRORS EVALUATION OF WEIGHING PLATFORMS WITH ARRANGEMENTS OF 2, 3 AND 4 FORCE SENSORS

Dmitrii Smirnov, Andrei Vorotnikov & Yuri Poduraev

This Publication has to be referred as: Smirnov, D[mitrii]; Vorotnikov, A[ndrei] & Poduraev, Y[uri]. Errors evaluation of weighing platforms with arrangements of 2, 3 and 4 force sensors, Proceedings of the 34th DAAAM International Symposium, pp.xxxx-xxxx, B. Katalinic (Ed.), Published by DAAAM International, ISBN 978-3-902734-xx-x, ISSN 1726-9679, Vienna, Austria
DOI: 10.2507/34th.daaam.proceedings.xxx

Abstract

Force sensors are used in many fields of activity as components for measuring forces applied to them or measuring weights installed on them. To measure the weight of large objects, weighing platforms are used, which require the mutual placement of several force sensors. When designing weighing platforms, it is necessary to implement solutions to various scientific problems. In particular, this is an increase in the measurement range of the platform while maintaining sensitivity. Or is it achieving greater stability of the weighing platform by increasing the number of support points. In addition, when installing force sensors in weighing platforms, additional errors arise due to the following factors: displacement of the position of the applied force on the platform relative to the measuring centre, inaccuracy of sensor installation (deviations in the shape and size of the surfaces of force sensors and the surfaces on which they are installed), as well as differences in the characteristics of the sensors. This paper discusses 3 sensor arrangements for the measuring platform: with 2, 3 and 4 force sensors respectively. An evaluation was made of the errors that arise when using these arrangements.

Keywords: force sensor; weighing platform; errors evaluation; sensor calibration

1. Introduction

Currently, force sensors are used for both domestic, industrial and medical purposes. Also in the development of robotics, force-torque sensing takes a special place [13]. Basically, it is needed either in joints of robots or on end-effector, as well as weighing platforms for studying robotic technological processes. Often, designs use several force sensors simultaneously to increase the range of measured values while maintaining sensitivity or to weigh large objects. For example, a common arrangement of sensors is a “rectangle”, where the sensors are located along the edges of the measuring platform, which makes it more stable (Fig. 1.a). This arrangement is quite widely used; examples include: floor platform, automobile or food scales. For example, work [9] describes the design of portable vehicle scales powered by solar energy for use in quarry conditions. In [10], this arrangement is used to weigh the hive, which helps beekeepers make observations. In [11], to assess the distribution of strawberry yield on a field, using a berry picking trolley equipped with a system of 4 force sensors.

In addition to this application, scientists are making attempts to use this arrangement for medical purposes. For example, as in work [2], where 4 force sensors are located at the edges of the bed under its legs and are used to determine the characteristics of human movements in sleep and their recognition based on sensor data. [3] integrated sensors into a hospital bed to monitor respiratory rate and tidal volume, and [4] described estimating a patient's heart rate using force sensors signals. Also, there are weighing platforms for monitoring the patient's gait, which use 6-component sensors to determine the magnitude and direction of forces and moments [5]. This article will discuss single-component single-point type sensors.

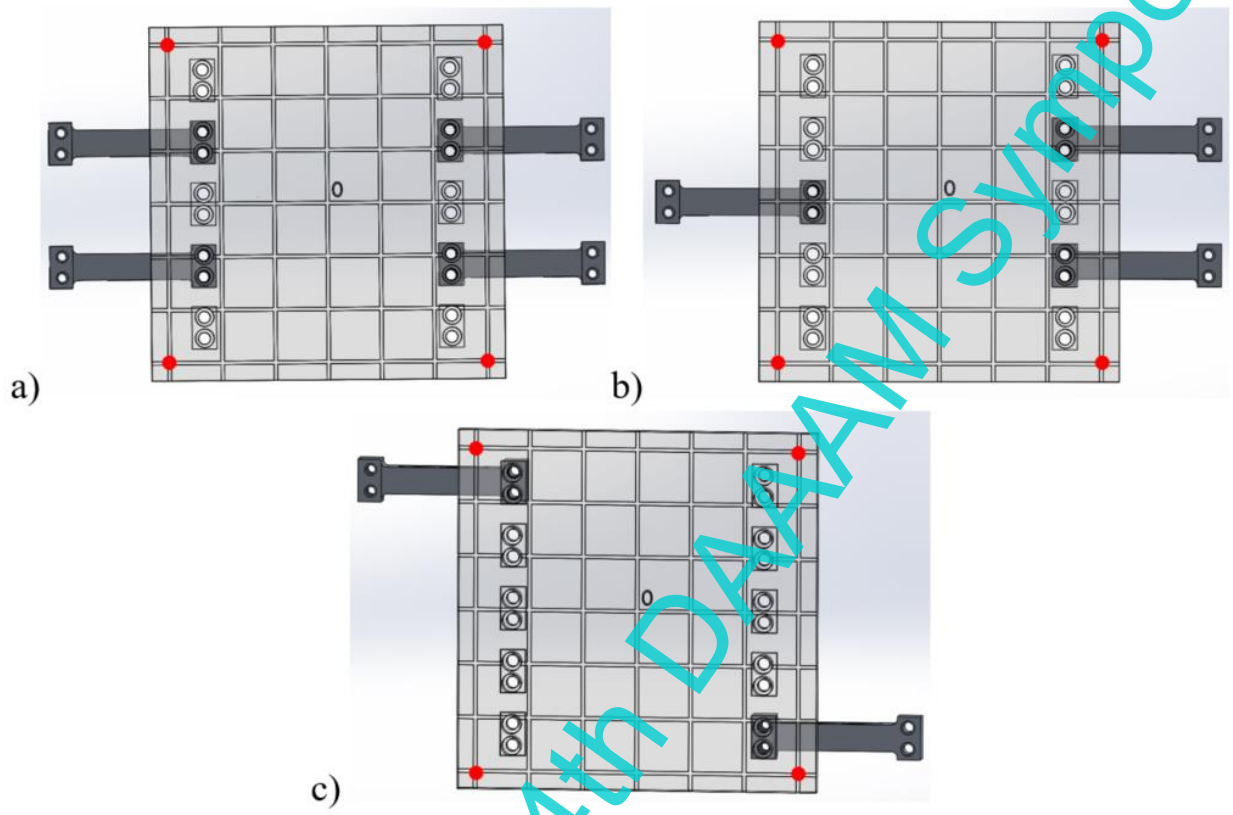

Fig. 1. Illustration of weighing platforms with arrangements of 2, 3 and 4 force sensors

The triangle design is often used to weigh bins of bulk materials, such as in [6] for a rice vending machine. However, an equilateral triangle is chosen, and the mass is always applied at the centre of this triangle. There is also an application for estimating engine thrust, where the air flow pressure is estimated using this arrangement [7]. In this work we will consider the diagram of an isosceles triangle (Fig. 1.b).

The final one is a diagram with two force sensors, the fastenings of which are located at the edges of the weighing platform (Fig. 1.c). This arrangement was used in [1] to determine the force acting on the motor rod. And also in the design of medical scales for weighing infants [8], where the error value of the eccentric application of force remained within the permissible error and amounted to 0.04% of the impact force at the nominal mass (+ - 2 grams with a nominal load capacity of the sensor of 10 kg).

The purpose of this work is to evaluate the errors of weighing platforms using several force sensors and the applicability of the considered arrangement s.

2. Materials and methods

To read voltages from force sensors, an ADS1256 analogue-to-digital converter is used, which has a 24-bit capacity and 8 channels, which allows you to connect 4 independent force sensors simultaneously and take their data with an accuracy of up to 298 nanovolts at a supply voltage of 5V. ADS1256 works in conjunction with Arduino Uno, which communicates with the ADC via the SPI interface for subsequent post-processing and transmission of measurement results to the serial port interface window. The schematic electrical diagram is shown in Figure 2. Post-processing consisted of converting the data from the ADC into voltage (mV) and, after calibration, into mass (grams). The reading frequency was 1 kHz. In order to minimize errors associated with spikes and conversion of analogue values using an ADC, average data over 400 values were evaluated.

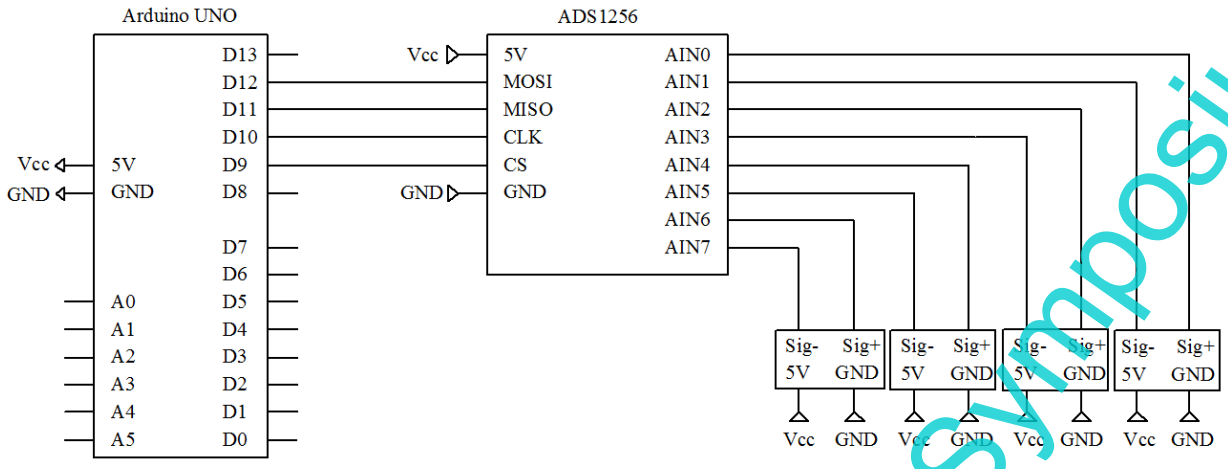

Fig. 2. Schematic diagram of connecting the components of the weighing platform

To conduct an evaluation of the errors of weighing platforms, it is necessary to have sensors that have been calibrated in order to correctly assess the resulting errors and compare them with the existing characteristics of the sensors. Therefore, the initial stage of scientific research was the calibration of each sensor separately. To do this, each sensor was gradually loaded up to 110% of the nominal load capacity, which is 100 grams, and unloaded using standard weights of accuracy class M1 (Fig. 3.). To obtain the coefficients for converting voltage, expressed in mV, into units of mass - grams, an approximation was carried out using the least squares method by the following minimization function:

$$\sum_{i=1}^{n}(U_i-(am_i+b))^2 \rightarrow \min$$

where U_i is the voltage from a separate sensor when applying mass m_i, where i is the index number of the measurement, n is the number of measurements, a and b are approximation coefficients.
As a result of calibration, the following sensor characteristics were obtained, shown in Table 1 below, for 2 cycles of 7 measurements during loading and unloading.

Number of sensors	**1**	**2**	**3**	**4**
Nominal load capacity [g]	100			
Zero balance %	0,027	0,033	0,008	0,005
Nonliniarity %	0,108	0,153	0,048	0,169
Hysteresis U %	0,045	0,014	0,010	0,072
Maximum deviation [g]	0,108	0,153	0,048	0,169
RCP mv/v	1,274	1,252	1,215	1,244
Standard deviation of sensor data after calibration from the applied mass [g]	0,029	0,042	0,013	0,054
Systematic error U%	0,031	0,076	0,009	0,133

Table 1. Sensor characteristics obtained as a result of calibration.

Figure 3 illustrates the calibration process force sensors using reference weights. Also, the right figure 3 shows the results for all sensors, where dots indicate experimental data, and solid colored lines show straight lines based on the found coefficients after the approximation.

As you can see, although the sensors are the same, they have different characteristics, which can affect the values measured by the weighing platform. When using certified sensors, these characteristics are indicated in the product passport or in the calibration certificate.

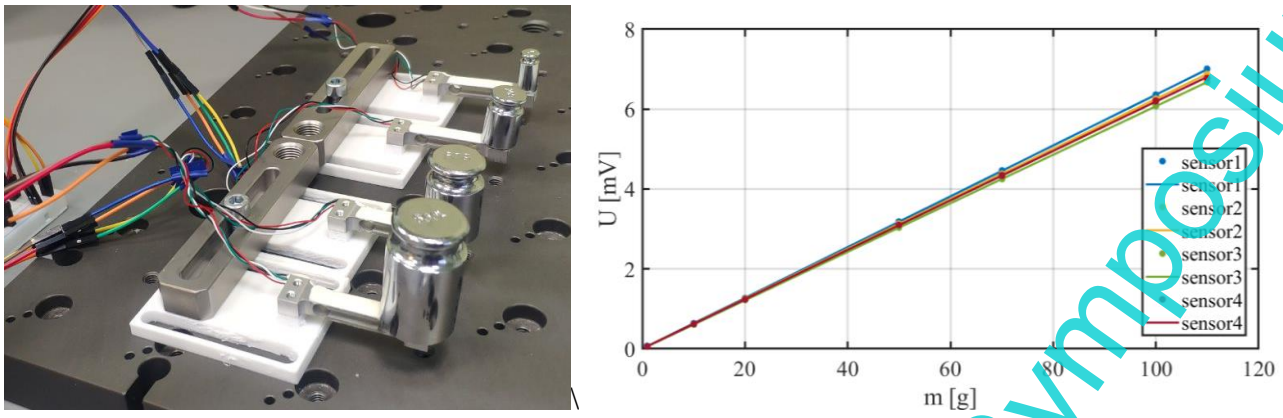

Fig.3. Calibration process using standard weights (left) and calibration curves obtained after fitting (right)

Initial calibration was also used during installation to ensure that the maximum permissible force on the sensor was not exceeded, which could lead to its failure. And also for leveling the platform, focusing on the data. After all, if the mass of the platform is evenly distributed across the sensors, then we can say that it is leveled.

When multiple sensors are used under one platform, the mass applied to it is distributed among the sensors. Accordingly, to evaluate the applied forces, it is necessary to add up the sensor data. Installation of sensors on the same platform makes them structurally interconnected, which leads to the appearance of a complex error, similar to that described in [12], i.e. consisting of several components:

$$F_{\Sigma} = \sum_{i=1}^{n} F_i + \Delta_{sen} + \Delta_{montage} + e$$

where F_{Σ} is the resulting force corresponding to the mass applied to the platform, taking into account errors (Δ_{sen} is the error caused by the presence of differences in the characteristics of the sensors, e is the eccentricity error (Fig. 4. on the right), caused by the displacement of the position of the weight on the measuring platform relative to the measuring centre, $\Delta_{montage}$ is the error arising due to deviations in the shape and size of the surfaces of the force sensors and the surfaces on which they are installed), F_i – data of the i-th sensor after calibration.

To evaluate the effect of the above errors, two experiments were carried out for all arrangement s. In the first it was assessed. To do this, the platform was sequentially loaded and unloaded in the same way as was done when calibrating each sensor separately earlier, it is important to note that the loads were located only in the centre of the platform. And in the second experiment, it was evaluated, where only a weight of 100 grams was used (which corresponds to the value of the nominal load capacity, in order to achieve the largest error value, since it was found that the error increases with increasing applied mass). For this purpose, a grid was outlined in advance (Fig. 1), at the intersection points of which (49 positions), weights were installed.

Based on the data obtained during the first experiment, the values of the maximum error and the standard deviation of the data of the resulting force of the sensors relative to the applied mass were calculated (Table 2). A similar assessment was carried out in [14]

Number of sensors	**2**	**3**	**4**
Maximum error [g]	3,6573	1,2615	0,5711
Standart diviation [g]	1,276	0,432	0,180

Table 2. Numerical values of the maximum error and standard deviation of the data of the resulting force of the sensors from the value of the applied mass for various sensor layouts

To reduce this error, the already assembled sensor system was recalibrated using the following algorithm:

1. Removing data in 4 extreme positions on the platform, indicated in Figure 1 and Figure 4 by red dots. – the value of the resulting force in the upper left position with coordinates (-3;3) when mi mass is applied; respectively – in the lower left (-3;-3), – in the lower right (3;-3), – in the upper right (3;3).
2. Approximation of average values from 4 positions relative to the applied mass mi using the least squares method:

$$\sum_{i=1}^{n}(\overline{F_{\Sigma_i}} - (a_\Sigma m_i + b_\Sigma))^2 \rightarrow \min$$

3. Entering the obtained coefficients a_Σ and b_Σ to obtain the resulting force corresponding to the mass applied to the platform:

$$F_{\Sigma cor} = \frac{(F_\Sigma - b_\Sigma)}{a_\Sigma}$$

This algorithm made it possible to reduce the influence of error. As a result, when installing weights in the centre of the platform, the following deviations were obtained, shown in Table 3. Which are comparable with the data given in Table 1.

Number of sensors	**2**	**3**	**4**
Maximum error [g]	0,2442	0,3624	0,2125
Standart deviation [g]	0,0532	0,0717	0,0666

Table 3. Numerical values of the maximum error and standard deviation of the data of the resulting force of the sensors from the value of the applied mass for various sensor layouts after recalibration

To evaluate the effect of error e, a second experiment was conducted. For this purpose, a weight weighing 100 g was used and was located at the intersection points of the intended grid on the platform (Fig. 1), which made it possible to visualize the distribution of error e relative to the average value from all positions on the platform (in order not to take into account the effect of other errors) depending on the location of the load on platform (Fig. 4).

$$e_j = F_{\Sigma j} - \overline{F_{\Sigma j}} \quad ,$$

where j is the serial number of the resulting force at different positions on the platform (marked purple in the fig- 4).

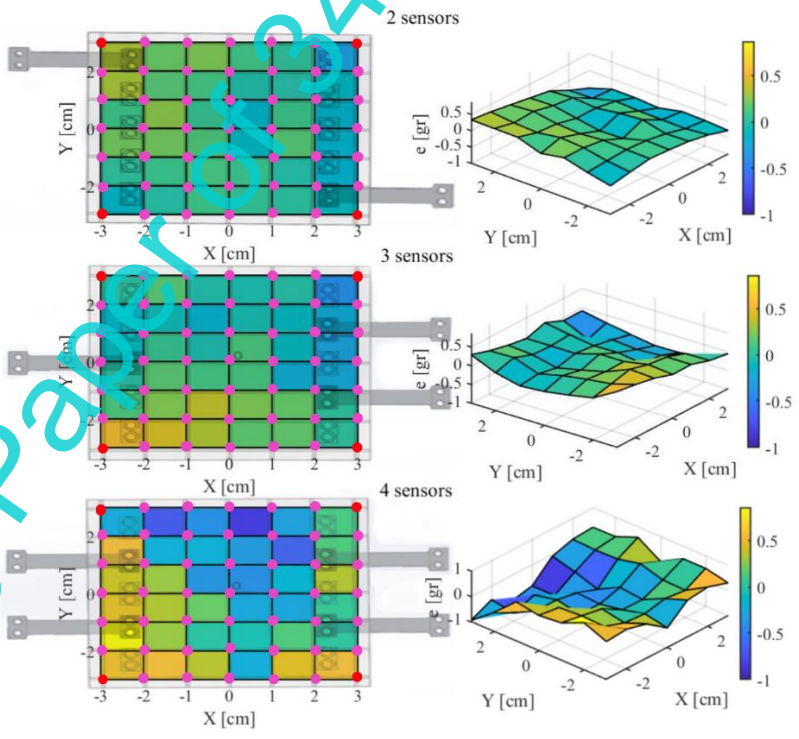

Fig. 4. Illustration of the distribution of error *e* relative to the average value from all positions on the platform depending on the location of the load for all arrangements.

The results show that a shift in the position of the weight on the measuring platform relative to the measuring centre leads to significant errors in the data up to 1 gram, which is 1% of the nominal load capacity of the sensors. Moreover, increasing the number of supports does not solve this problem, but on the contrary leads to an increase in error. It is important that the resulting error is unevenly distributed over the measuring surface. The relationship between the distribution of this error and the geometric dimensions between the supports will be investigated in future work. After all, if we identify the systematic component of such a phenomenon, then it will be possible to design weighing systems of any size with a sense of the error with which they will carry out measurements.

3. Conclusion

In this work, various arrangements of 2, 3 and 4 force sensors for weighing platforms were considered. In the course of the work, it was found that the error that occurs when several sensors are used together, the connection between each other is constructive, complex and conditional, takes into account the following factors: placing weight measurements on the measuring platform relative to the measuring centre, inaccuracy of sensor measurements (deviations in the shape and size of the characteristics force sensors and the characteristics they provide), as well as differences in sensor characteristics. The first will be considered in subsequent works: the study of the error arising due to the displacement of dimensions relative to the centre depending on the geometric dimensions between the supports, which will make it possible to design weighing platforms with the size of this error. The second can lead to the creation of additional bending moments, leading to increased errors and a more labour-intensive assembly process. Supposedly, the performance issue can be corrected by using additional soft spacers, which will be tested in subsequent work. The latter error introduced by analogue conversions in sensor characteristics can be reduced by retransmission after the sensor system has been assembled. It can also be said that the presented diagrams represent consistency for use.

4. References

[1] Belitsky E., Solovyev M., Kovalsky V., Vorotnikov A., Kordonsky A., Grin A., Poduraev Yu. (2023) “Mechatronic linear movement device for constructing surfaces of complex shapes with the possibility of force measurement”, Robotics and Technical Cybernetics. No. 11 (2)., pp. 85-93. DOI: 10.31776/rtcj.11201 – Text: electronic.

[2] Adami, A. M., Hayes, T. L., Pavel, M., & Singer, C. M. (2006, January). Detection and classification of movements in bed using load cells. In 2005 IEEE Engineering in Medicine and Biology 27th Annual Conference (pp. 589-592). IEEE..

[3] Jung, H., Kimball, J. P., Receveur, T., Gazi, A. H., Agdeppa, E. D., & Inan, O. T. (2022). Estimation of tidal volume using load cells on a hospital bed. IEEE Journal of Biomedical and Health Informatics, 26(7), 3330-3341.

[4] Jung, H., Kimball, J. P., Receveur, T., Agdeppa, E. D., & Inan, O. T. (2021). Accurate ballistocardiogram based heart rate estimation using an array of load cells in a hospital bed. IEEE Journal of Biomedical and Health Informatics, 25(9), 3373-3383.

[5] Payton, C. J., & Burden, A. (Eds.). (2017). Biomechanical evaluation of movement in sport and exercise: the British Association of Sport and Exercise Sciences guide. Routledge.

[6] Yuliandoko, H., Panduardi, F., Lusi, N., & Wibowo, S. (2023, February). Precision Rice Vending Machine by Using Multiple Load Cell and IoT Based. In 2023 International Conference on Computer Science, Information Technology and Engineering (ICCoSITE) (pp. 296-300). IEEE.

[7] Baer, P. H. (2008). 3 Load Cell Tumble Meter Development (No. 2008-01-3004). SAE Technical Paper.

[8] Новиков, Ю. С., & Ситдиков, Ф. Г. (2001). Весы медицинские электронные. // Novikov Yu. S.& Sitdikov F. G. (2001) Medical electronic scales.

[9] Zamri, N. S. M., Mohamad, K. A., Alias, A., Razali, E. F., & Nordin, M. S. (2022). Development of A Solar-Powered Weighbridge System Using Load Cells in Quarry Site. Evolution in Electrical and Electronic Engineering, 3(1), 402-408..

[10] Zacepins, A., Pecka, A., Osadcuks, V., Kviesis, A., & Engel, S. (2017). Solution for automated bee colony weight monitoring. Agronomy Research, 15(2).

[11] Anjom, F. K., Vougioukas, S. G., & Slaughter, D. C. (2018). Development and application of a strawberry yield-monitoring picking cart. Computers and electronics in agriculture, 155, 400-411.

[12] Vorotnikov, A. A., Poduraev, Y. V., & Romash, E. V. (2015). Estimation of error in determining the centres of rotation of links in a kinematic chain for industrial robot calibration techniques. Measurement Techniques, 58, 864-871.

[13] Solovyev, M., Andrei, V., Klimov, D., Vladislav, K., & Poduraev, Y. (2017). Control system of the Articulated Arm Braking Mechatronic Machine (AABMM). Annals of DAAAM & Proceedings, 28.

[14] Vorotnikov, A., Romash, E., Isaev, A., Bashevskaya, O., Bianchi, G., & Poduraev, Y. (2016, January). Uncertainty estimation of axes direction determination of industrial robot using an ellipsoid concentration model. In Proceedings of the 27th DAAAM International Symposium (pp. 0480-0486).